^{18}F-FDG PET Scanning in Pulmonary Amyloidosis

Misbah Baqir[1], Val Lowe[2], Eunhee S. Yi[3], and Jay H. Ryu[1]

[1]Division of Pulmonary and Critical Care Medicine, Mayo Clinic, Rochester, Minnesota; [2]Department of Diagnostic Radiology, Mayo Clinic, Rochester, Minnesota; and [3]Division of Anatomic Pathology, Mayo Clinic, Rochester, Minnesota

^{18}F-FDG PET plays an important role in the evaluation of patients with lung malignancies but can lead to false-positive and false-negative results. Very little is known about ^{18}F-FDG PET scanning in amyloidosis. **Methods:** A computer-assisted search of medical records was conducted to identify subjects with pulmonary amyloidosis (confirmed by biopsy) who were seen at the Mayo Clinic during a 15-y period between January 1, 1997, and December 31, 2011, and had a PET scan available for current review. **Results:** Eighteen patients were diagnosed to have amyloidosis by lung biopsy (15 surgical, 2 transthoracic needle, and 1 bronchoscopic). The mean age of the patients was 64.8 y (range, 32–80 y). Seventeen patients had primary amyloidosis, including 5 with Sjögren syndrome, 1 with rheumatoid arthritis, and 1 with multiple myeloma. The most common abnormal findings on the chest CT scan were pulmonary nodules (n = 14), followed by cysts (n = 6) and reticular opacities (n = 4). Eight patients had positive ^{18}F-FDG PET results (intrathoracic ^{18}F-FDG uptake), including 4 patients with coexisting mucosa-associated lymphoid tissue lymphoma (maximal standardized uptake value [SUVmax] range, 3.1–6.7) and 1 patient with a pleural plasmacytoma (SUVmax, 7.2); the remaining 3 patients had amyloid only (SUVmax range, 2.1–3.2). Ten patients with negative PET results included 3 additional patients with mucosa-associated lymphoid tissue lymphoma. **Conclusion:** Positive ^{18}F-FDG PET results, especially with an SUVmax of more than 3, in patients with pulmonary amyloidosis should raise suspicion about associated lymphoma or plasmacytoma, but negative PET results do not exclude the presence of such neoplasms.

Key Words: amyloidosis; lymphoma, B-cell, marginal zone; positron-emission tomography; pulmonary nodule; Sjögren's syndrome

J Nucl Med 2014; 55:565–568
DOI: 10.2967/jnumed.113.130823

Amyloidosis refers to a group of conditions that result from extracellular deposition of insoluble fibrillar protein and can be systemic or organ-limited (localized) (*1,2*). A variety of precursor proteins can form insoluble amyloid fibrils of β-pleated sheet structure that allows the characteristic binding of Congo red stain (*2,3*). Amyloidosis can be acquired or inherited, and the 3 most common forms are primary amyloidosis (immunoglobulin light chains), transthyretin amyloidosis, and amyloid A protein amyloidosis. Clinical manifestations of amyloidosis are diverse and determined by the type of precursor protein, tissue distribution, and extent of deposition (*2*).

Pulmonary involvement in amyloidosis can be classified as tracheobronchial disease, parenchymal nodules, localized or diffuse interstitial infiltrates, intrathoracic lymphadenopathy, and pleural disease (*4,5*). Pulmonary amyloidosis is usually due to primary amyloidosis and can be difficult to diagnose (*4,5*). Sometimes the presentation can resemble a malignancy, particularly when it presents with pulmonary nodules, intrathoracic lymphadenopathy, or pleural effusion.

^{18}F-FDG PET is extensively used in the evaluation of known or suspected lung cancer. However, ^{18}F-FDG PET has limitations in diagnostic accuracy, and it is recognized that false-positive ^{18}F-FDG PET results can be seen in various nonmalignant disorders. Very little is known about ^{18}F-FDG PET scanning in amyloidosis. In this study, we sought to characterize ^{18}F-FDG PET findings in patients with pulmonary amyloidosis.

MATERIALS AND METHODS

Patient Selection

A computer-aided search was conducted to identify all adults (at least 18 y old) who were seen at the Mayo Clinic during a 15-y period between January 1, 1997, and December 31, 2011, and were diagnosed on lung biopsy to have pulmonary amyloidosis (187 patients). Of these patients, we identified 18 who had undergone ^{18}F-FDG PET scanning. The major indication for ^{18}F-FDG PET scanning was concern about malignancy, especially in patients with pulmonary nodules, and evaluation for possible metastatic disease. The Mayo Foundation Institutional Review Board approved this retrospective study (study identification number 10-006289), and the requirement to obtain informed consent was waived. Patients who did not authorize the use of their medical records for research were excluded.

Clinical, Laboratory, and Radiologic Findings

Data extracted from the medical records included age, sex, smoking status, primary symptoms, method of diagnosis, pathologic findings including the type of amyloid, spirometric results, findings on chest CT scans, and findings on ^{18}F-FDG PET scans.

^{18}F-FDG PET Imaging

All PET scans were reviewed for the purposes of this study by a nuclear medicine specialist without knowledge of the clinical and pathologic data, and the mean maximum standardized uptake value (SUVmax) was determined. Lesions with ^{18}F-FDG uptake greater than uptake in the blood pool and with SUVmax levels above 2.0 were considered positive, taking into consideration the visual appearance of the activity distribution: whether it was focal (more likely malignant) or diffuse (more likely inflammatory). ^{18}F-FDG PET imaging was performed according to our standard clinical practice (Advance PET tomograph or DRX/690 combined PET/CT scanner; GE Healthcare). ^{18}F-fluoride was produced on site (Trace Cyclotron; GE

Received Aug. 12, 2013; revision accepted Oct. 28, 2013.
For correspondence or reprints contact: Jay H. Ryu, Division of Pulmonary and Critical Care Medicine, Gonda 18 South, Mayo Clinic, 200 First St. SW, Rochester, MN 55905.
E-mail: ryu.jay@mayo.edu
Published online Feb. 20, 2014.

TABLE 1
Demographic, Clinical, and Radiologic Features of 18 Subjects with Pulmonary Amyloidosis

Characteristic	Data
Male sex	9 (50)
Age (y)	
Mean ± SD	64.8 ± 13.1
Median	69.5
Range	32–80
Smoking status	
Current	2 (11)
Previous	4 (22)
Never	12 (67)
Presenting symptoms	
Dyspnea	6 (33)
Cough	5 (28)
Fatigue	2 (11)
None	8 (44)
CT findings	
Nodules	14 (78)
Cysts	6 (33)
Interstitial/septal thickening	4 (22)
Bronchiectasis	3 (17)
Lymphadenopathy	3 (17)
Pleural effusion	3 (17)
Emphysema	3 (17)
Pulmonary function*	
Obstruction	6 (43)
Restriction	1 (7)
Reduced DLCO only	1 (7)
Normal	6 (43)

*Pulmonary function results were not available in 4 of 18 subjects.

DLCO = carbon monoxide diffusion in lung.

Data are *n* followed by percentage in parentheses, except for age.

Healthcare). ^{18}F-FDG synthesis was performed by the standard method, and the product was tested for sterility, pyrogenicity, and radiochemical purity on each production run. PET images of the body to include the infracranial head, neck, chest, and abdomen to at least the level of the iliac crest were obtained 60 min after intravenous injection of 559–740 MBq of ^{18}F-FDG. After voiding, the patients were positioned on the tomographic gantry for imaging. Emission images were processed using iterative reconstruction. Attenuation correction was used on all data. Emission data were corrected for scatter, random events, and dead-time losses using the manufacturer's software. The image pixel size was 4.25 mm displayed in a 128 × 128 mm array. Standard orthogonal views, as well as maximum-intensity projections, were reviewed during scan interpretation. CT scan fusion was available on the images obtained by the combined PET/CT scanner (DRX/690; GE Healthcare).

RESULTS

The mean age of the 18 subjects with pulmonary amyloidosis was 64.8 y (range, 32–80 y); they included an equal number of men and women (Table 1). There were 12 never-smokers and 6 with a smoking history (including 2 current smokers). Ten subjects were symptomatic, most commonly with dyspnea with or without cough, but 8 subjects were evaluated for abnormalities noted on chest imaging in the absence of relevant symptoms. Fourteen patients underwent pulmonary function testing, and 8 had abnormal findings, with airflow obstruction being the most common pattern of abnormality. Among 6 patients with airflow obstruction, 4 had a smoking history. Echocardiography was performed on 11 patients, of whom 2 were found to have echocardiographic findings consistent with amyloid heart disease.

Seventeen of 18 patients had primary amyloidosis; in the remaining patient, with an isolated pulmonary amyloidoma (1.1-cm solitary pulmonary nodule), the type of amyloid could not be determined. Associated conditions included Sjögren syndrome (n=5), multiple myeloma (n = 1), and rheumatoid arthritis (n= 1). The most common findings on high-resolution CT scans of the chest were nodules (n = 14), followed by cysts (n = 6) and reticular opacities (n = 4) (Fig. 1A).

Fifteen patients were diagnosed by surgical lung biopsy, 2 by transthoracic needle biopsy, and 1 by bronchoscopic biopsy. Seven patients (39%) were found to have a mucosa-associated lymphoid tissue (MALT) lymphoma along with amyloid deposits. Eight patients had positive ^{18}F-FDG PET results (intrathoracic ^{18}F-FDG uptake) (Table 2), including 4 patients with associated MALT lymphoma (SUVmax range, 3.1–6.7) (Fig. 1B) and 1 patient with a pleural plasmacytoma (SUVmax, 7.2). The remaining 3 patients had amyloid only (SUVmax range, 2.1–3.2). Ten patients with negative ^{18}F-FDG PET results included 3 additional patients with associated MALT lymphoma, whereas the remaining 7 patients had amyloid only. This resulted in a sensitivity of 63% and specificity of 70% for ^{18}F-FDG PET in diagnosing lymphoplasmacytic neoplasms in patients with pulmonary amyloidosis.

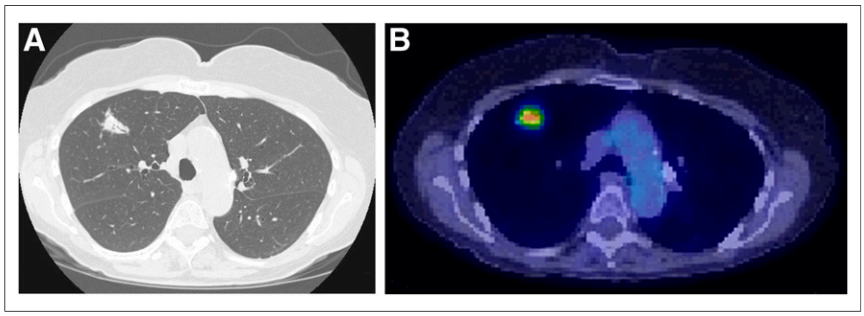

FIGURE 1. Images of 78-y-old woman with Sjögren syndrome. (A) High-resolution CT scan of chest demonstrates irregular nodule measuring 2.4 × 1.2 cm and containing air bronchograms in right upper lobe. On resection, nodule proved to be MALT lymphoma with plasmacytic differentiation and associated amyloid. (B) ^{18}F-FDG PET scan demonstrates increased uptake of ^{18}F-FDG (SUVmax, 6.7) in right-upper-lobe nodule.

DISCUSSION

In this study of 18 patients with pulmonary amyloidosis undergoing ^{18}F-FDG PET scanning, 8 (44%) exhibited increased intrathoracic ^{18}F-FDG uptake, among whom more than half had an associated lymphoplasmacytic neoplasm, that is, lymphoma or plasmacytoma. However, 3 additional patients with intrathoracic MALT lymphoma displayed negative results on ^{18}F-FDG PET scanning.

Pulmonary amyloidosis is usually due to primary amyloidosis with deposition of immunoglobulin light-chain fragments (*5*). A broad array of intrathoracic manifestations

TABLE 2
Characteristics of 8 Subjects with Positive ^{18}F-FDG PET Findings

Age (y)	Sex	CT findings	Lung biopsy	Lung pathology	Location of ^{18}F-FDG uptake	SUVmax
64	F	Multiple nodules	Transthoracic needle	MALT lymphoma with plasmacytic differentiation, amyloid	Multiple nodules	5.2
78	F	Nodule with satellite nodularity	Surgical	MALT lymphoma with plasmacytic differentiation, amyloid	Single nodule	6.7
67	M	Multiple nodules, mediastinal and hilar adenopathy	Surgical	Nodular amyloid	Multiple nodules and intrathoracic lymph nodes	2.1
73	F	Multiple nodules, bronchiectasis	Surgical	MALT lymphoma with plasmacytic differentiation, amyloid	Single nodule	5.7
69	F	Interstitial/septal thickening, pleural mass	Bronchoscopic; transthoracic needle	Interstitial amyloid; plasmacytoma with amyloid	Pleural mass (plasmacytoma)	7.2
54	F	Multiple nodules	Surgical	Nodular amyloid	Single nodule	3.2
75	F	Multiple cysts, nodules	Bronchoscopic	Amyloid	Single nodule	2.6
75	M	Nodule	Surgical	MALT lymphoma with plasmacytic differentiation, amyloid	Single nodule	3.1

is associated with amyloidosis, ranging from tracheobronchial parenchymal (consolidation, nodular, cystic, and interstitial) and pleural involvement to mediastinal and hilar lymphadenopathy (*4*). The most common manifestation is parenchymal nodules as seen in our study. These nodules raise suspicion about malignancy (either primary lung cancer or metastatic disease). Moreover, pulmonary involvement in amyloidosis can be associated with lymphoproliferative disorders such as MALT lymphoma, which is usually associated with an indolent clinical course (*6*).

^{18}F-FDG PET, which is based on functional rather than morphologic mapping, plays an important role in the assessment and management of many types of malignancy. The role of ^{18}F-FDG PET scanning in patients with amyloidosis has been unclear, with only a few case reports relevant to this issue having been published (*3,7–12*). In addition, the few retrospective studies that have been published on the role of ^{18}F-FDG PET in patients with MALT lymphoma have yielded conflicting results (*13–17*).

In the current study of 18 patients with biopsy-proven pulmonary amyloidosis, the most common CT findings were pulmonary nodules. Among 10 patients who had amyloidosis only (without MALT lymphoma or plasmacytoma), 3 exhibited positive ^{18}F-FDG PET results, although the SUVmax tended to be lower than that seen in patients with lymphoma or plasmacytoma. Among 5 patients with lymphoplasmacytic neoplasm, the range of SUVmax was 3.1–7.2, whereas 3 additional patients showed no ^{18}F-FDG uptake.

Hoffmann et al. (*15*) suggested that the degree of ^{18}F-FDG uptake for MALT lymphoma may be explained on the basis of underlying histology, that is, plasma cell differentiation. In their study, the sensitivity of ^{18}F-FDG PET was 83% for plasmacytically differentiated MALT lymphoma, as compared with 20% for typical MALT lymphoma. The fact that there is a high likelihood that a ^{18}F-FDG PET scan will be positive in multiple myeloma also supports this theory related to plasma cell differentiation (*18*). Another case report supported this theory when, after treatment with the monoclonal anti-CD20 antibody rituximab, there was high focal uptake on an ^{18}F-FDG PET scan of a patient with MALT lymphoma. This finding was attributed to rituximab's causing complete elimination of marginal-zone cells, resulting in overgrowth of the plasmacytic component (*19*).

There were several limitations to our study, including the retrospective design and a modest number of study subjects. Although the sensitivity and specificity of ^{18}F-FDG PET scanning in detecting lymphoid neoplasm was 63% and 70%, respectively, the accuracy of these values is admittedly uncertain given the small sample size. The patients with amyloidosis undergoing ^{18}F-FDG PET scanning consisted mainly of those with parenchymal nodules or intrathoracic lymphadenopathy, that is, suspected of malignancy. Nonetheless, our results provide some additional insights into the potential role of ^{18}F-FDG PET scanning in patients with pulmonary amyloidosis.

CONCLUSION

Our results provide additional insights into the interpretation of ^{18}F-FDG PET results in patients with pulmonary amyloidosis. Increased uptake of ^{18}F-FDG, particularly with an SUVmax greater than 3, increases suspicion about an associated lymphoma or plasmacytoma. On the other hand, negative PET results do not exclude the presence of such neoplasms.

DISCLOSURE

The costs of publication of this article were defrayed in part by the payment of page charges. Therefore, and solely to indicate this fact, this article is hereby marked "advertisement" in accordance

with 18 USC section 1734. No potential conflict of interest relevant to this article was reported.

REFERENCES

1. Picken MM. Amyloidosis: where are we now and where are we heading? *Arch Pathol Lab Med.* 2010;134:545–551.
2. Merlini G, Seldin DC, Gertz MA. Amyloidosis: pathogenesis and new therapeutic options. *J Clin Oncol.* 2011;29:1924–1933.
3. Sideras K, Gertz MA. Amyloidosis. *Adv Clin Chem.* 2009;47:1–44.
4. Sharma OP. Paraproteinemias and the lungs. *Curr Opin Pulm Med.* 2005;11:408–411.
5. Lachmann HJ, Hawkins PN. Amyloidosis and the lung. *Chron Respir Dis.* 2006;3:203–214.
6. Jeong YJ, Lee KS, Chung MP, et al. Amyloidosis and lymphoproliferative disease in Sjögren syndrome: thin-section computed tomography findings and histopathologic comparisons. *J Comput Assist Tomogr.* 2004;28:776–781.
7. Currie GP, Rossiter C, Dempsey OJ, Legge JS. Pulmonary amyloid and PET scanning. *Respir Med.* 2005;99:1463–1464.
8. Yadav S, Sharma S, Gilfillan I. Unusual positron emission tomography findings in pulmonary amyloidosis: a case report. *J Cardiothorac Surg.* 2006;1:32.
9. Grubstein A, Shitrit D, Sapir EE, Cohen M, Kramer MR. Pulmonary amyloidosis: detection with PET-CT. *Clin Nucl Med.* 2005;30:420–421.
10. Tan H, Guan Y, Zhao J, Lin X. Findings of pulmonary amyloidosis on dual phase FDG PET/CT imaging. *Clin Nucl Med.* 2010;35:206–207.
11. Soussan M, Ouvrier M-J, Pop G, Galas J-L, Neuman A, Weinmann P. Tracheobronchial FDG uptake in primary amyloidosis detected by PET/CT. *Clin Nucl Med.* 2011;36:723–724.
12. Ollenberger GP, Knight S, Tauro AJ. False-positive FDG positron emission tomography in pulmonary amyloidosis. *Clin Nucl Med.* 2004;29:657–658.
13. Beal KP, Yeung HW, Yahalom J. FDG-PET scanning for detection and staging of extranodal marginal zone lymphomas of the MALT type: a report of 42 cases. *Ann Oncol.* 2005;16:473–480.
14. Alinari L, Castellucci P, Elstrom R, et al. ^{18}F-FDG PET in mucosa-associated lymphoid tissue (MALT) lymphoma. *Leuk Lymphoma.* 2006;47:2096–2101.
15. Hoffmann M, Wohrer S, Becherer A, et al. ^{18}F-fluoro-deoxy-glucose positron emission tomography in lymphoma of mucosa-associated lymphoid tissue: histology makes the difference. *Ann Oncol.* 2006;17:1761–1765.
16. Perry C, Herishanu Y, Metzer U, et al. Diagnostic accuracy of PET/CT in patients with extranodal marginal zone MALT lymphoma. *Eur J Haematol.* 2007;79:205–209.
17. Zhang WD, Guan YB, Li CX, Huang XB, Zhang FJ. Pulmonary mucosa-associated lymphoid tissue lymphoma: computed tomography and ^{18}F fluorodeoxyglucose-positron emission tomography/computed tomography imaging findings and follow-up. *J Comput Assist Tomogr.* 2011;35:608–613.
18. Mulligan ME. Imaging techniques used in the diagnosis, staging, and follow-up of patients with myeloma. *Acta Radiol.* 2005;46:716–724.
19. Woehrer S, Streubel B, Chott A, Hoffmann M, Raderer M. Transformation of MALT lymphoma to pure plasma cell histology following treatment with the anti-CD20 antibody rituximab. *Leuk Lymphoma.* 2005;46:1645–1649.